Nano Energy (2015) 12, 588–596

Available online at www.sciencedirect.com

ScienceDirect

journal homepage: www.elsevier.com/locate/nanoenergy

RAPID COMMUNICATION

# Piezotronic effect enhanced detection of flammable/toxic gases by ZnO micro/nanowire sensors

Ranran Zhou[a,1], Guofeng Hu[a,1], Ruomeng Yu[b,1], Caofeng Pan[a,*], Zhong Lin Wang[a,b,*]

[a]Beijing Institute of Nanoenergy and Nanosystems, Chinese Academy of Sciences, Beijing 100083, China
[b]School of Materials Science and Engineering, Georgia Institute of Technology, Atlanta, GA 30332-0245, USA

Received 23 December 2014; received in revised form 21 January 2015; accepted 22 January 2015
Available online 2 February 2015

**KEYWORDS**
Piezotronic effect;
Flammable/toxic gas sensors;
ZnO micro/nanowire;
Schottky-contact;
Room-temperature

**Abstract**
Compared with conventional Ohmic-contact nanosensors, Schottky-contact has been introduced as a fundamentally new design for much enhanced sensitivity and improved responsive time of one-dimensional nanostructure based sensors. Here we demonstrate ZnO micro/nanowire sensors for hydrogen ($H_2$) and nitrogen dioxide ($NO_2$) detections at room-temperature based on a metal-semiconductor-metal (M-S-M) structure. By utilizing strain-induced piezoelectric polarization charges presented at the vicinity of local interface to modify the band structure at Schottky contact, piezotronic effect has been introduced to gate/modulate the charge carriers transport process across the M-S contact and thus hugely enhance/optimize the performances of $H_2$/$NO_2$ gas sensors. Upon straining, the detection sensitivity and resolution are obviously improved, together with a significant enhancement in output current by 5359% for $H_2$ and 238.8% for $NO_2$ detection. This work provides a promising approach to raise the sensitivity, improve the detection resolution, and generally enhance the performance of gas sensing, making it possible for fabricating room temperature of gas sensor while preserving its sensitivity.


## Introduction

Monitoring and quantifying the amount of flammable/toxic gas in the ambient environment is of great importance to both personal and environmental safeties. Especially for those

*Corresponding authors.
*E-mail addresses:* cfpan@binn.cas.cn (C. Pan), zlwang@gatech.edu (Z.L. Wang).
[1]Authors contributed equally to this work.

http://dx.doi.org/10.1016/j.nanoen.2015.01.036
2211-2855/

colorless, odorless and tasteless hazardous gases such as hydrogen ($H_2$) or poisonous and irritant gases such as nitrogen dioxide ($NO_2$), it is essential to detect them quantitatively to prevent potential explosion or poisoning, since general human senses cannot distinguish their presences. One-dimensional (1D) nanostructures such as nanowires [1,2], nanorods [3] and nanobelts [4,5] have been extensively investigated for ultra-sensitive and fast-response gas sensing [6–9] due to their unique structural characteristics and versatile physical properties, such as high volume-to-surface ratio and short-transport path for carriers. Although promising results have been reported for Ohmic-contact nanosensors for gas detections [10–12], further improvements on the sensing performances remain challenging since the manipulation and fabrication process become extremely difficult and expensive when miniaturizing the nanostructure to ensure small contact areas. Low-cost and easy-fabricated Schottky-contact structure nanosensor, on the other hand, is considered as a prospective alternate for gas sensing applications with ultra-high sensitivity and fast response time, since the sensing functionality depends on interfacial carrier transport, which is a more effective and sensitive working mechanism [13].

Piezotronic effect [14], usually existing in wurtzite/zinc blend family materials, has been recently reported as an efficient approach to directly gate the transport properties of the carrier in the semiconductor [15,16] or to tune/control the Schottky barrier height (SBH) through modifying the band structure at local M–S contacts upon straining [17–19]. The strain-induced piezoelectric polarization charges presented at the vicinity of local interface effectively gate/modulate the charge carriers transport process across the energy barrier, and thus enhance/optimize the performances of Schottky-contact structured nanosensors of various categories, including chemical [20,21], biological [22], optical [23,24] and humidity sensing [25]. Therefore, piezotronic effect is universal to different types of Schottky-contact sensors as an effective approach to improve the sensitivity and enhance/optimize their general performances.

In this work, we designed and fabricated Schottky-contact ZnO micro/nanowire sensors for flammable/toxic gas detections. By surface decorating the ZnO nanowire (NW) with Pd nanoparticles for catalytic dissociation of $H_2$ to atomic hydrogen [26,27], hydrogen detection is demonstrated since the adsorbed hydrogen atoms acting as donors to induce a charge accumulation layer on the NW surface [28], and thus increasing the carrier density within n-type ZnO NWs. By exposing ZnO NW devices to $NO_2$ atmosphere, the strong oxidizing $NO_2$ molecules act as electron acceptors, are easily to bind in the preferential adsorption sites provided by the oxygen vacancies at the oxide surface and are more inclined to capture electrons from the conduction band and form $NO_2^-$ [29]. Subsequently, a charge depletion layer produced near the surface [30], which effectively decreases the conductivity of the device. Piezotronic effect is introduced by externally applying strains to the ZnO micro/nanowire sensors to enhance/optimize their performances. Experimental results show that the detection sensitivity and resolution are obviously improved; the output current is significantly enhanced by 5359% for $H_2$ and 238.8% for $NO_2$ detection. Strain-induced piezo-polarization charges play an essential role in modifying the band structure at M–S contact and hence gating the charge carrier transport process across the Schottky barrier. This study provides a promising approach to improve the detection sensitivity and enhance the general performance of Schottky-contact gas sensors, making it possible for fabricating room-temperature gas sensor while preserving its sensitivity.

## Experimental section

### ZnO micro/nanowire synthesis and characterization

ZnO micro/nanowires were synthesized *via* vapor-liquid-solid (VLS) method [31,32]. An alumina boat (3.5 cm × 6.5 cm) loaded with a mixture of 1 g ZnO and 1 g carbon powders was placed in the center of a tube furnace, a silicon substrate coated with 5 nm Au was placed on the top of the alumina boat with the Au layer facing down. The typical synthesis procedure was carried out at a temperature of 1000 °C with the flow rate of nitrogen gas at 100 standard cubic centimeters per minute (sccm) for 1 h. The ZnO micro/nanowires were characterized by SEM (SU8020). After the ZnO synthesis process, Pd nanoparticles were fabricated by radio frequency (RF) sputtering at room temperature. The ZnO micro/nanowires substrate was deposited in a vacuum chamber with the flow rate of argon at 100 sccm, with RF power of 100 W for 20 s.

### Device fabrication

The single micro/nanowire gas sensor was fabricated by transferring and bonding an individual ZnO/Pd or ZnO micro/nanowire onto a flexible polystyrene (PS) substrate, with its *c*-axis parallel to the longitudinal direction of the PS substrate. Then silver paste was used to fix both ends of the micro/nanowire and also served as source and drain electrodes.

### Measurement and piezotronic effect on a single micro/nanowire gas sensor

One end of the as-fabricated device was fixed inside the gas chamber. The other end of the device was free to be bent by a positioner controlled from outside the chamber with a displacement resolution of 1 μm.

For $H_2$ detection, high concentration hydrogen gas (800 ppm) diluted with nitrogen gas was introduced to the sensor in appropriate concentrations through mass flow controller (BEQ, GMF-3Z), with the total flow rate fixed at 100 sccm. The sensing performance of the device was studied at room temperature by measuring the current changes of the device when switching the sensing chamber environment from air to $H_2$ in a periodic manner, with $H_2$ concentration ranging from 80 to 320 ppm. *I–V* characteristics of the device at different strains in gas environment with different $H_2$ concentrations were recorded through Stanford research systems (SR570 and DS345).

For $NO_2$ measurement, high concentrations $NO_2$ gas (800 ppm) diluted with nitrogen gas was introduced into the chamber through mass flow controller (BEQ, GMF-3Z), with the flow rate fixed at 100 sccm. The sensing performance of the device was studied in the same method as that used for $H_2$ detection, with $NO_2$ concentration ranging from 160 to 800 ppm.

## Results and discussion

High-quality ZnO micro/nanowires used in this work were grown by a vapor-liquid-solid process at 1000 °C, with lengths of several hundreds of microns and diameters varying from tens of nanometers to several microns (Fig. 1a). An enlarged SEM image of an individual ZnO NW is shown as the inset of Fig. 1a. Schematic illustrations of the experimental setup are presented in Fig. 1b, showing that one end of the device is fixed inside the chamber, while the other end is free to be bent by a positioner through a 3D mechanical stage with movement resolution of 1 μm. An optical image of the as-fabricated ZnO micro/nanowire gas sensor is shown in the inset of Fig. 1b, with detailed fabrication process described in the aforementioned part. The response of ZnO micro/nanowire sensors to flammable/toxic gas is evaluated by measuring its transport characteristics under different gas concentrations at room temperature, with bias voltage fixed at 3 V for $H_2$ sensor and 5 V for $NO_2$ sensor, respectively.

The current response of a Pd-functionalized ZnO micro/nanowire $H_2$ sensor is presented in Fig. 1c. By varying the hydrogen concentrations inside the measuring chamber, the current of the sensor increases stepwise with the hydrogen concentrations from 0.56 μA (80 ppm) to 0.82 μA (320 ppm), showing a sensitive response to the hydrogen atmosphere changes. The response time is about 100 s, the recovery time is about 10 s. There is a slightly current increase in $N_2$ atmosphere, which is consistent with the expected surface electron-depletion layer created by the chemisorbed oxygen species on the surface of the ZnO in air [13]. The observed response and recover properties of the Pd-functionalized $H_2$ sensor are mainly contributed to the "spillover effect" reported previously by others [33]. Performances of a ZnO micro/nanowire $NO_2$ sensor are shown in Fig. 1d, which is obtained by applying a 253.7 nm UV illumination for 10 min before the measurements to pre-remove the oxygen adsorbed on the ZnO surface. The current decreases with the increase of the $NO_2$ concentration from 3.20 μA (160 ppm) to 2.87 μA (800 ppm). The response time is about 60 s, and the recovery time is about 30 s. It can be seen that the current incompletely recovers to the original level after evacuating the $NO_2$ in each cycle, indicating a partial desorption and decomposition process of the main adsorbed nitrates [34]. UV light is employed for assisting the current recovery of $NO_2$ sensors to original level more effectively [35].

Systematic measurements of ZnO micro/nanowire gas sensors response to $H_2$ and $NO_2$ are conducted and summarized in Fig. 2 *via I-V* characteristics at room temperature. Among air, 80 ppm and 320 ppm $H_2$ atmosphere, the Pd-functionalized $H_2$ sensors are measured under different strain conditions, showing increase in output current by either introducing more $H_2$ or applying more strains (Fig. 2a-c). For example, under strain-free condition (Fig. 2a-c, black line), the current of the gas sensor increases from 0.074 μA to 0.23 μA, then to 0.61 μA as the test environment

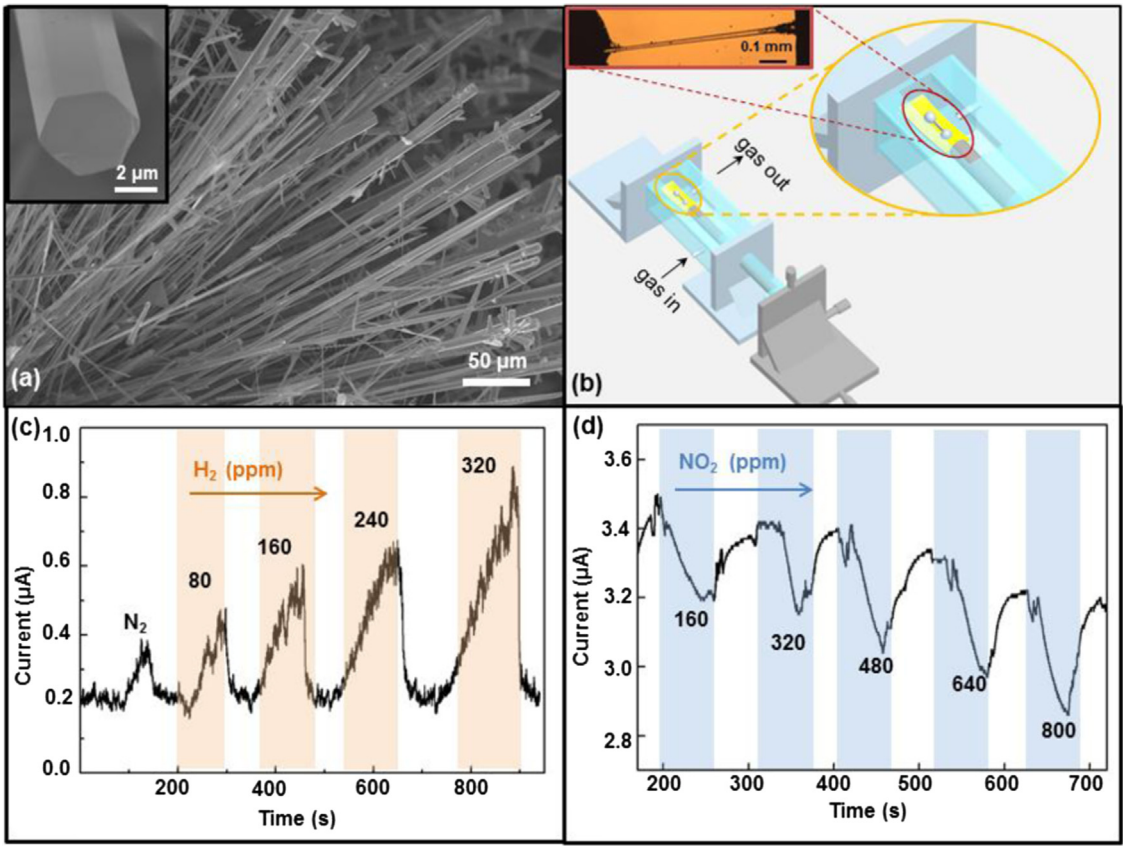


**Fig. 1** (a) Scanning electron microscopy (SEM) images of the as-grown ZnO NWs.(b) Schematic illustration of the experimental setups. Inset: the optical image of an as-fabricated gas sensor device. (c) Current response of a Pd-functionalized $H_2$ sensor to different hydrogen concentrations.(d) Current response of a $NO_2$ sensor to different $NO_2$ concentrations.

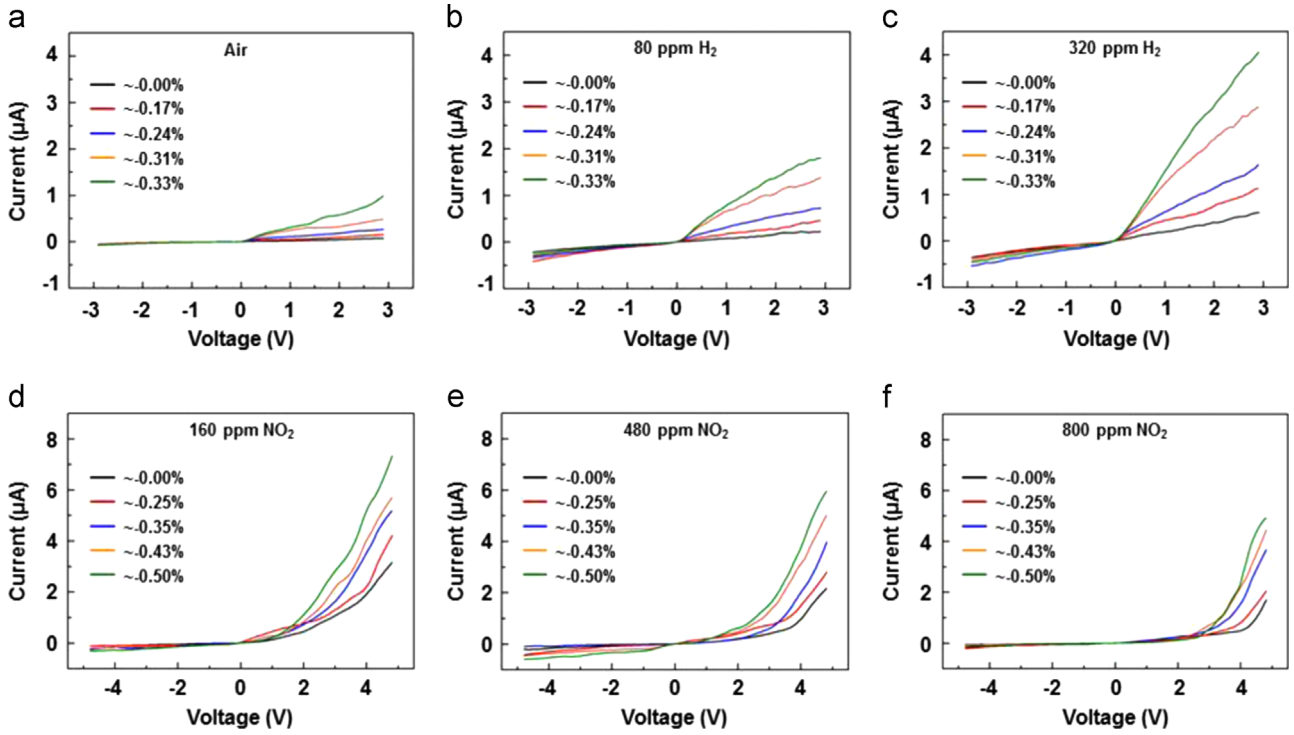


**Fig. 2** General $H_2$ and $NO_2$ sensing performances. (a-c) *I-V* characteristics of the $H_2$ sensor under different compressive strains (a) in air; (b) 80 ppm and (c) 320 ppm $H_2$ atmosphere. (d-f) *I-V* characteristics of the $NO_2$ sensor under different compressive strains in (d) 160 ppm, (e) 480 ppm and (f) 800 ppm $NO_2$ atmosphere.

changes from air to 80 ppm $H_2$ and then to 320 ppm $H_2$, showing a good hydrogen response of the device. In air atmosphere, the current increases from 0.074 μA to 0.94 μA (by 1170%) as the applied compressive strain varying from −0.00% to −0.33% (Fig. 2a). In 320 ppm $H_2$ atmosphere, the current increases from 0.61 μA to 4.05 μA (by 564%) as the compressive strain changing from −0.00% to −0.33% (Fig. 2c). These results clearly show the significant enhancements in output current of ZnO micro/nanowire sensors under compressive strains by piezotronic effect.

Similar responses are derived for $NO_2$ detection as shown in Fig. 2d-f. Under strain-free condition, the current decreases from 2.88 μA to 2.10 μA and then to 1.47 μA, as the $NO_2$ concentration increases from 160 ppm to 480 ppm then to 800 ppm (Fig. 2d-f, black line). In 160 ppm $NO_2$ atmosphere, the current increases from 2.88 μA (−0.00% strain) to 7.19 μA (−0.50% strain), corresponding to an enhancement of 149.7% (Fig. 2d). In 800 ppm $NO_2$ atmosphere, the current increases from 1.47 μA (−0.00% strain) to 4.98 μA (−0.50% strain) with a relative change of 238.8% as shown in Fig. 2f. The enlarged output currents in different $NO_2$ atmosphere significantly facilitate the detection and clearly indicate the enhancements induced by piezotronic effect under externally applied compressive strains.

A 3D plot is presented in Fig. 3a to indicate the overall trend of current response to $H_2$ atmosphere and externally applied strain conditions for hydrogen detection, clearly showing that the current increases with the increase of $H_2$ concentration or compressive strain. Two corresponding 2D graphs are plotted in Fig. 3b and c to illustrate the enhancements on detecting sensitivity and sensing resolutions by piezotronic effect after applying external strains. Fig. 3b presents the absolute current response of Pd-functionalized $H_2$ sensors to different $H_2$ concentrations, with compressive strain fixed in each curve, ranging from −0.00% to −0.33%. The detection sensitivity of $H_2$ sensors are characterized by the slope of each curve, showing higher sensitivity under stronger compressive strains. Fig. 3c shows the current response of $H_2$ sensors to different strains, with $H_2$ concentrations fixed in each curve (from 0 to 320 ppm). The sensing resolution is clearly improved by piezotronic effect under compressive strains, since the difference of current response between two adjacent $H_2$ concentrations is increased by applying more compressive strains on the devices.

To better illustrate the enhancements on detection sensitivity of hydrogen sensors by piezotronic effect, the relative current change of the Pd-functionalized $H_2$ sensor in different $H_2$ concentration and strain conditions is calculated and summarized in Fig. 3d and e, by defining the detection sensitivity as $dI/I=(I_{\text{hydrogen},\ \varepsilon}-I_0)/I_0$, where $I_0$ is the current in air atmosphere under strain-free condition, and $I_{\text{hydrogen},\ \varepsilon}$ is the current under certain $H_2$ concentration and strain conditions. It is obvious that the detection sensitivity under each $H_2$ concentration is significantly enhanced by piezotronic effect through applying compressive strains on the devices, with the highest sensitivity of 5359% in 320 ppm $H_2$ atmosphere, under −0.33% compressive strain (Fig. 3e). These results agree well with the increase in curve slope (Fig. 3b) and indicate the obvious enhancements on detection sensitivity of hydrogen sensors by piezotronic effect. Similar enhancements on detection sensitivity and sensing resolutions are also observed and presented in Fig. 4 for $NO_2$ sensors. Both the slope of *I* vs. $NO_2$ concentration curves and the difference between output currents corresponding to two adjacent $NO_2$ concentrations

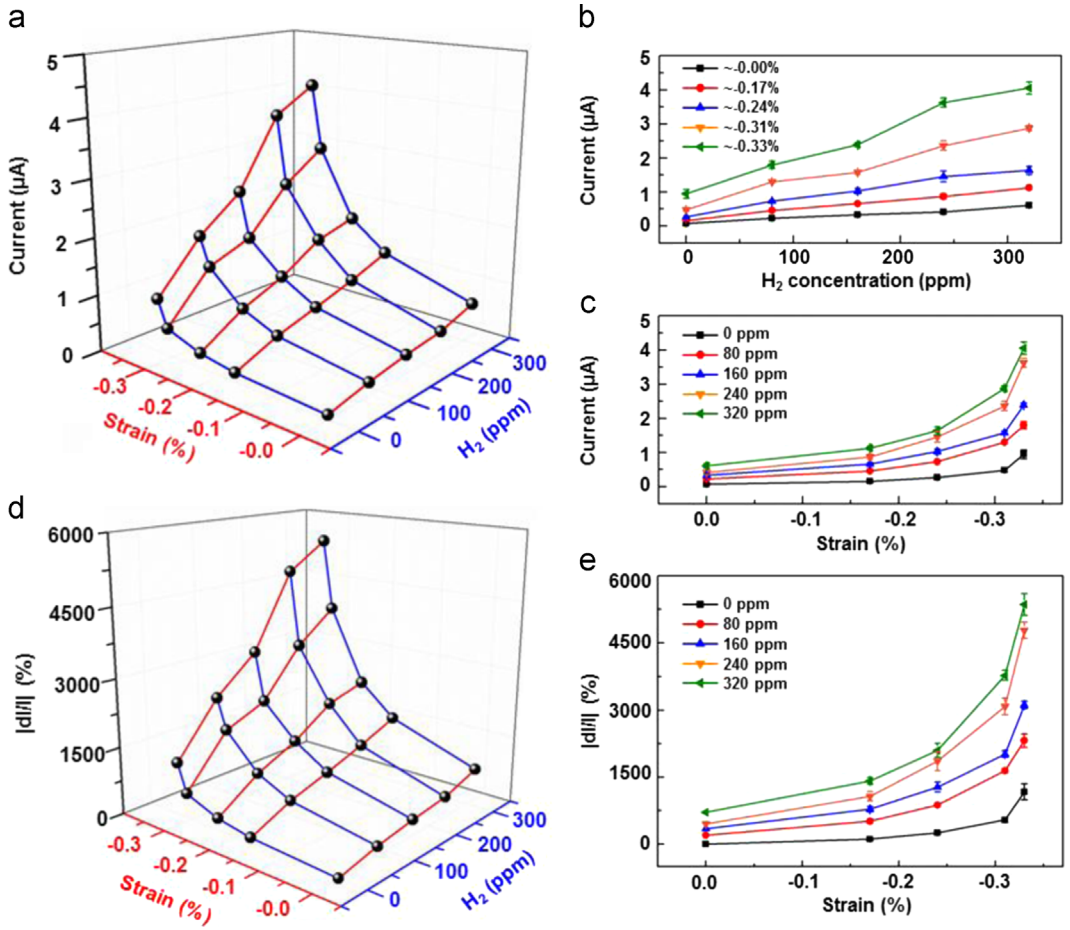


**Fig. 3** Piezotronic enhancements on $H_2$ sensing. (a) 3D graph depicting the current response of the $H_2$ sensor to strain and $H_2$ concentrations at a bias voltage of 2.9 V. (b) Absolute current response to different $H_2$ concentrations, with compressive strains ranging from −0.00% to −0.33%. (c) Absolute current response to different compressive strains, with $H_2$ concentrations ranging from 0 to 320 ppm. (d)3D graph and its corresponding (e) 2D projection indicating the relative changes of current under $H_2$ concentrations ranging from 0 to 320 ppm with respect to the value at −0.00% strain in air.

increase when applying more compressive strains, indicating the improvements to the performances of ZnO micro/nanowire based $NO_2$ sensors by piezotronic effect.

The barrier height at reversely biased Schottky contact ($\Phi_d$) and the corresponding resistances of ZnO NWs are calculated by utilizing a Matlab GUI program [36] build on an equivalent model for the M-S-M structure. In a Schottky diode under moderate bias, the current density is given by the following equation:

$$J = \frac{A \times T\sqrt{\pi E_{00}}}{k} \times \sqrt{q(V-\varepsilon) + \frac{\psi}{\cos h^2\left(\frac{E_{00}}{kT}\right)}} \times \exp\left(-\frac{\psi}{E_0}\right) \times \exp\left(\frac{qV}{kT} - \frac{qV}{E_0}\right)$$

where $\psi$ is the effective SBH, $V$ is the applied bias, $\varepsilon$ is the distance between the Fermi level to the bottom of the conduction band, $T$ is the temperature, and $A$ is Richardson constant. The constants $E_0$ and $E_{00}$ are given by the following equation:

$$E_0 = E_{00} \coth\left(\frac{E_{00}}{kT}\right)$$

$$E_{00} = \frac{\hbar q}{2} \times \sqrt{\frac{N_d}{m^* \varepsilon_s \varepsilon_0}}$$

where $m^*$ is the effective mass, $N_d$ is the doping concentration and $\varepsilon_s, \varepsilon_0$ are the relative permittivity of the ZnO NW and the absolute permittivity of free space. In the M-S-M structure, a linear region is expected in the *I-V* curve at large bias. The resistance of the ZnO NW can thus be determined from the linear region *via*:

$$R_{ns} \approx \frac{dV}{dI}|_{\text{large bias}}$$

By fitting the *I-V* characteristics derived from ZnO micro/nanowire sensors under different atmosphere and strain conditions (Fig. 2) with this GUI program, the Schottky barrier heights at drain electrode ($\Phi_d$) are simulated and summarized in Fig. 5a and b for $H_2$ and $NO_2$ detections, respectively. As the reversely biased Schottky contact, the value of $\Phi_d$ effectively dominates the charge carriers transport process across the local interface [37,38]. Fig. 5a presents the SBH $\Phi_d$ in air, 80 ppm and 320 ppm hydrogen atmosphere under different strain conditions based on the experiment data presented in Fig. 2a-c; Fig. 5b

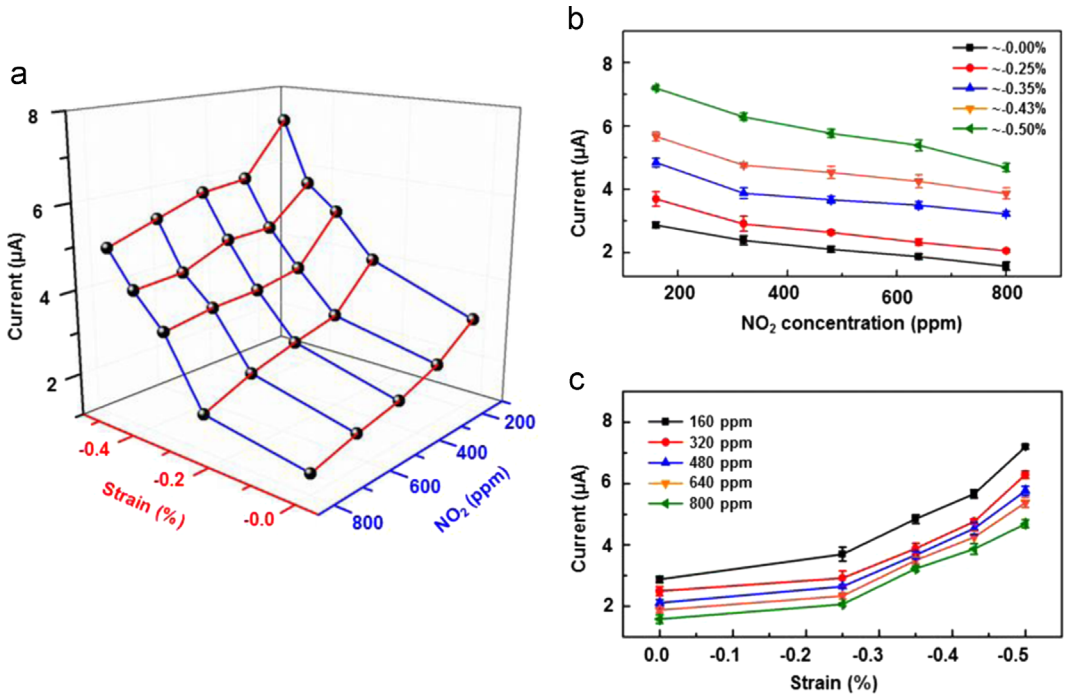


**Fig. 4** Piezotronic enhancements on $NO_2$ sensing. (a) 3D graph depicting the current response of the $NO_2$ sensor to strain and $NO_2$ concentrations at a bias voltage of 4.8 V. (b) Absolute current response to different $NO_2$ concentrations, with compressive strains ranging from −0.00% to −0.50%. (c) Absolute current response to different compressive strains, with $NO_2$ concentrations ranging from 160 to 800 ppm.

shows the $\Phi_d$ in 160, 480 and 800 ppm $NO_2$ atmosphere under different strain conditions based on the experiment data presented in Fig. 2d-f. Both simulation results indicate obvious decrease of $\Phi_d$ as applying more compressive strains on the devices under each measurement atmosphere, corresponding to the enhancement of output current for both $H_2$ and $NO_2$ detections by piezotronic effect. Accordingly, the resistances of ZnO NWs are calculated and presented in Fig. 5c and d, showing consistency with the changes of $\Phi_d$ and also decreasing as increasing the externally applied compressive strains. These results agree well with the previous reports on gas sensing devices [39-42].

Band diagrams of ZnO NWs are carefully analyzed as shown in Fig. 6 to illustrate the physical working mechanism of ZnO $H_2/NO_2$ sensors and their piezotronic effect enhanced performances. A Schottky contact is formed at local M-S contact (reversely biased drain electrode) in air as shown in Fig. 6a. Once introducing hydrogen gas into the chamber, the adsorbed hydrogen molecules dissociate on the catalytic Pd nanoparticles by reacting with pre-existing $O_2^-$ and releasing the trapped electrons to the conduction band of ZnO. Therefore, hydrogen molecules serve as donors by injecting electrons into ZnO conduction band to induce an accumulation layer of charge carriers on the surface of ZnO NW (Fig. 6c) and thus increase the conductivity and output current of the device. By introducing $NO_2$ gas into the chamber, the strong oxidizing $NO_2$ molecules interact with the oxygen vacancies or zinc interstitial [43] and become negatively charged units by draining electrons from the conduction band of ZnO. This process reduces the number of free electrons inside ZnO NW and leads to a depletion layer [29] near the surface (Fig. 6e), decreasing the conductivity and output current of the ZnO micro/nanowire gas sensor [30]. Upon straining, based on the crystal orientation of ZnO (c-axis pointing from drain to source electrode) and the polarity of strains (compressive strains), positive piezoelectric polarization charges [37] are induced at the local M-S contact (Fig. 6b, d and f) and effectively reduce the barrier height of reversely biased Schottky contact. Thus piezotronic effect is employed to modify the band structure at M-S interface and contribute to the enhancements on output current as well as the general performances of ZnO micro/nanowire gas sensors.

## Conclusion

In summary, we designed and fabricated flexible Schottky-contact ZnO micro/nanowire sensors for flammable/toxic gas detections. Both hydrogen ($H_2$) and nitrogen dioxide ($NO_2$) detections are demonstrated at room-temperature based on M-S-M structured devices. By utilizing strain-induced piezoelectric polarization charges presented at the vicinity of local interface to modify the band structure at Schottky contact, piezotronic effect has been introduced to gate/modulate the charge carriers transport process across the M-S contact and thus enhance/optimize the performances of $H_2/NO_2$ gas sensors. Upon straining, the detection sensitivity and resolution are obviously improved, together with a significant enhancement in output current by 5359% for $H_2$ and 238.8% for $NO_2$ detection. Band diagrams of ZnO NWs are carefully investigated to illustrate the working

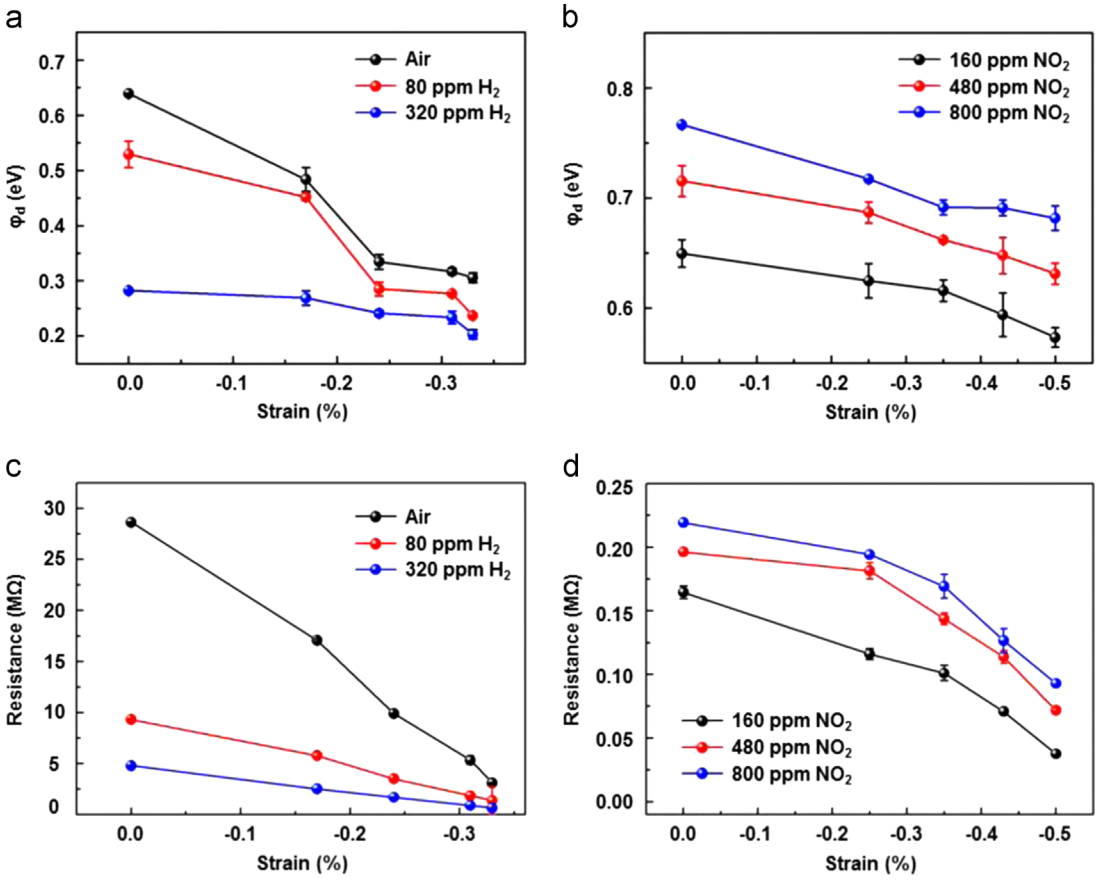


**Fig. 5** Theoretical simulations of ΔSBH and Resistance. (a-b)The fitting results of SBH $\Phi_d$ changes with compressive strains ranging from (a) −0.00% to −0.33% for $H_2$ sensing; (b) −0.00% to −0.50% for $NO_2$ sensing. (c-d) The fitting results of NW resistance changes with compressive strains ranging from (c) −0.00% to −0.33% for $H_2$ sensing; (d) −0.00% to −0.50% for $NO_2$ sensing.

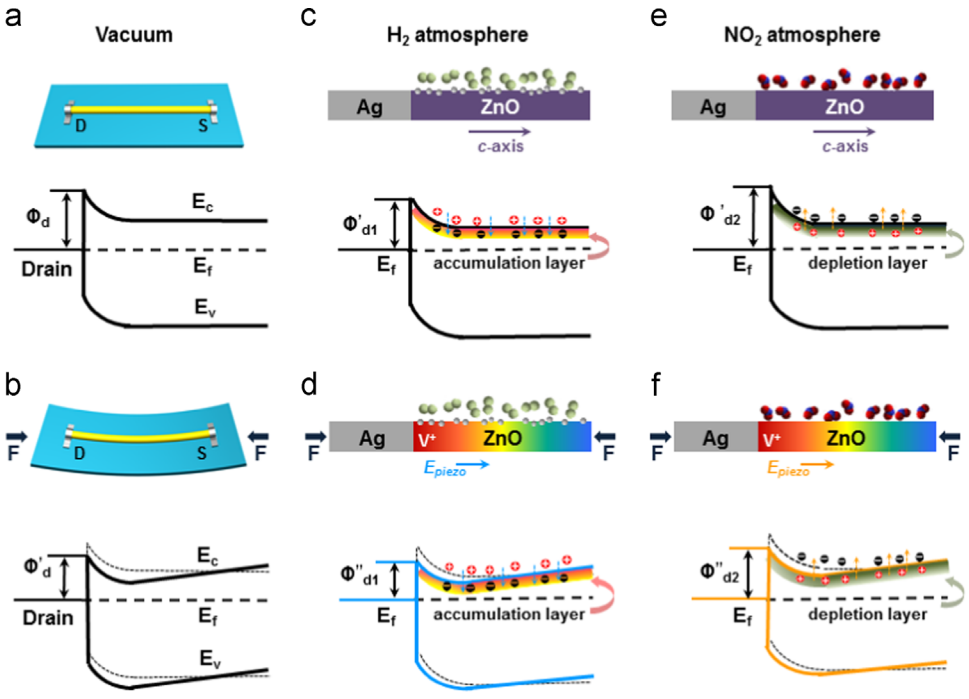


**Fig. 6** Working mechanism. Schematic energy band diagrams of ZnO NW in (a) vacuum; (b) vacuum under compressive strains; (c) $H_2$ atmosphere; (d) $H_2$ atmosphere under compressive strains; (e) $NO_2$ atmosphere; (f) $NO_2$ atmosphere under compressive strains.

principle and the enhancement mechanism by piezotronic effect for $H_2/NO_2$ detections. This work provides a promising approach to raise the sensitivity, improve the detection resolution, and generally enhance the performance of Schottky-contact micro/nanowire gas sensors.

## Acknowledgements

The authors are grateful for the support from the "Thousands Talents" program for pioneer researcher and his innovation team, China; President Funding of the Chinese Academy of Sciences; National Natural Science Foundation of China (No.51272238, 21321062, 51432005 and 61405040); the Beijing Municipal Science & Technology Commission (Z131100006013004, Z131100006013005).

## References

[1] Y. Cui, Q.Q. Wei, H.K. Park, C.M. Lieber, Science 293 (2001) 1289–1292.
[2] Q. Kuang, C. Lao, Z.L. Wang, Z. Xie, L. Zheng, J. Am. Chem. Soc. 129 (2007) 6070–6071.
[3] H. Huang, Y.C. Lee, O.K. Tan, W. Zhou, N. Peng, Q. Zhang, Nanotechnology 20 (2009).
[4] X.Y. Kong, Z.L. Wang, Nano Lett. 3 (2003) 1625–1631.
[5] Z.W. Pan, Z.R. Dai, Z.L. Wang, Science 291 (2001) 1947–1949.
[6] A. Kolmakov, Y. Zhang, G. Cheng, M. Moskovits, Adv. Mater. 15 (2003) 997–1000.
[7] C.S. Rout, K. Ganesh, A. Govindaraj, C.N.R. Rao, Appl. Phys. A—Mater. Sci. Process. 85 (2006) 241–246.
[8] F. Yang, S.-C. Kung, M. Cheng, J.C. Hemminger, R.M. Penner, ACS Nano 4 (2010) 5233–5244.
[9] Q.H. Li, Y.X. Liang, Q. Wan, T.H. Wang, Appl. Phys. Lett. 85 (2004) 6389–6391.
[10] P. Offermans, M. Crego-Calama, S.H. Brongersma, Nano Lett. 10 (2010) 2412–2415.
[11] Y. Cheng, P. Xiong, L. Fields, J.P. Zheng, R.S. Yang, Z.L. Wang, Appl. Phys. Lett. 89 (2006) 093114.
[12] P. Andrei, L.L. Fields, J.P. Zheng, Y. Cheng, P. Xiong, Sens. Actuators, B—Chem. 128 (2007) 226–234.
[13] T.Y. Wei, P.H. Yeh, S.Y. Lu, Z. Lin-Wang, J. Am. Chem. Soc. 131 (2009) 17690–17695.
[14] Z.L. Wang, Nano Today 5 (2010) 540–552.
[15] L. Chen, M.-C. Wong, G. Bai, W. Jie, J. Hao, Nano Energy (2014). http://dx.doi.org/10.1016/j.nanoen.2014.11.039.
[16] G. Bai, M.-K. Tsang, J. Hao, Adv. Opt. Mater. (2014). http://dx.doi.org/10.1002/adom.201400375.
[17] X.D. Wang, J. Zhou, J.H. Song, J. Liu, N.S. Xu, Z.L. Wang, Nano Lett. 6 (2006) 2768–2772.
[18] J. Zhou, Y.D. Gu, P. Fei, W.J. Mai, Y.F. Gao, R.S. Yang, G. Bao, Z.L. Wang, Nano Lett. 8 (2008) 3035–3040.
[19] P.H. Yeh, Z. Li, Z.L. Wang, Adv. Mater. 21 (2009) 4975–4978.
[20] C.F. Pan, R.M. Yu, S.M. Niu, G. Zhu, Z.L. Wang, ACS Nano 7 (2013) 1803–1810.
[21] R.M. Yu, C.F. Pan, J. Chen, G. Zhu, Z.L. Wang, Adv. Funct. Mater. 23 (2013) 5868–5874.
[22] R.M. Yu, C.F. Pan, Z.L. Wang, Energ. Environ. Sci. 6 (2013) 494–499.
[23] Q. Yang, X. Guo, W.H. Wang, Y. Zhang, S. Xu, D.H. Lien, Z.L. Wang, ACS Nano 4 (2010) 6285–6291.
[24] R.M. Yu, C.F. Pan, Y.F. Hu, L. Li, H.F. Liu, W. Liu, S. Chua, D.Z. Chi, Z.L. Wang, Nano Res. 6 (2013) 758–766.
[25] G.F. Hu, R.R. Zhou, R.M. Yu, L. Dong, C.F. Pan, Z.L. Wang, Nano Res. 7 (2014) 1083–1091.
[26] R. Nowakowski, R. Dus, Langmuir 19 (2003) 6750–6758.
[27] H.T. Wang, B. Kang, F. Ren, L. Tien, P. Sadik, D. Norton, S. Pearton, J. Lin, Appl. Phys. Lett. 86 (2005) 243503.
[28] T.B. Fryberger, S. Semancik, Sens. Actuators, B—Chem. 2 (1990) 305–309.
[29] A.Z. Sadek, S. Choopun, W. Wlodarski, S.J. Ippolito, K. Kalantar-Zadeh, IEEE Sens. J. 7 (2007) 919–924.
[30] Y. Shimizu, M. Egashira, MRS Bull. 24 (1999) 18–24.
[31] X.D. Wang, C.J. Summers, Z.L. Wang, Nano Lett. 4 (2004) 423–426.
[32] G. Zhu, Y.S. Zhou, S.H. Wang, R.S. Yang, Y. Ding, X. Wang, Y. Bando, Z.L. Wang, Nanotechnology 23 (2012).
[33] A. Kolmakov, D.O. Klenov, Y. Lilach, S. Stemmer, M. Moskovits, Nano Lett. 5 (2005) 667–673.
[34] M. Chen, Z. Wang, D. Han, F. Gu, G. Guo, J. Phys. Chem. C 115 (2011) 12763–12773.
[35] M. Law, H. Kind, B. Messer, F. Kim, P.D. Yang, Angew. Chem. Int. Ed. 41 (2002) 2405–2408.
[36] Y. Liu, Z.Y. Zhang, Y.F. Hu, C.H. Jin, L.M. Peng, J. Nanosci. Nanotechnol. 8 (2008) 252–258.
[37] R.M. Yu, L. Dong, C.F. Pan, S.M. Niu, H.F. Liu, W. Liu, S. Chua, D.Z. Chi, Z.L. Wang, Adv. Mater. 24 (2012) 3532–3537.
[38] Z.L. Wang, Adv. Mater. 19 (2007) 889–892.
[39] C. Baratto, G. Sberveglieri, A. Onischuk, B. Caruso, S. di Stasio, Sens. Actuators, B—Chem. 100 (2004) 261–265.
[40] J.H. Jun, J. Yun, K. Cho, I.-S. Hwang, J.-H. Lee, S. Kim, Sens. Actuators, B—Chem. 140 (2009) 412–417.
[41] M.W. Ahn, K.S. Park, J.H. Heo, D.W. Kim, K.J. Choi, J.G. Park, Sens. Actuators, B—Chem. 138 (2009) 168–173.
[42] T.-R. Rashid, D.-T. Phan, G.-S. Chung, Sens. Actuators, B—Chem. 193 (2014) 869–876.
[43] M. Epifani, J.D. Prades, E. Comini, E. Pellicer, M. Avella, P. Siciliano, G. Faglia, A. Cirera, R. Scotti, F. Morazzoni, J. R. Morante, J. Phys. Chem. C 112 (2008) 19540–19546.

**Ranran Zhou** is a master student from 2013 under the guidance of Prof. Caofeng Pan in Beijing Institute of Nanoenergy and Nanosystems (BINN), Chinese Academy of Science, China. She received her B.S. degree in Materials science and engeneering from Zhengzhou University in 2013. Her current research interest is physical and chemical processes in nanomaterials growth, properties, fabrication of novel devices, and their unique applications in sensing systems and energy science.

**Guofeng Hu** received the B.S. degree in School of Science from Tianjin Polytechnic University, China, in 2010. He is currently pursuing the Ph.D. degree at the Laboratory of piezo-phototronics, Beijing Institute of Nanoenergy and Nanosystems, Chinese Academy of Sciences. His research work is focusing on the fields of piezotronics/piezo-phototronics for fabricating new electronic and optoelectronic devices.

**Ruomeng Yu** is a Ph.D. candidate in School of Materials Science and Engineering at Georgia Institute of Technology, under the supervision of Prof. Zhong Lin Wang as a graduate research assistant. He received his B.S. degree in Applied Physics from Huazhong University of Science and Technology in 2010, and his M.S. degree in Physics from Georgia Institute of Technology in 2012. His research interests include synthesis, fabrication and integration

of nanomaterials/electronic devices; nano/micro-scale electronics for energy harvesting/conversion/storage; self-powered sensing systems; mechanical/optical signals-controlled logic circuits; optoelectronics; piezotronics/piezo-photonics/piezo-phototronics.

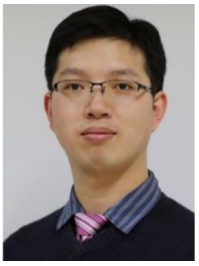

**Dr. Caofeng Pan** received his B.S. degree (2005) and his Ph.D. (2010) in Materials Science and Engineering from Tsinghua University, China. He then joined in the group of Professor Zhong Lin Wang at the Georgia Institute of Technology as a postdoctral fellow. He is currently a professor and a group leader at Beijing Institute of Nanoenergy and Nanosystems, Chinese Academy of Sciences since 2013. His main research interests focus on the fields of piezotronics/piezo-phototronics for fabricating new electronic and optoelectronic devices, nano-power source (such as nanofuel cell, nano biofuel cell and nanogenerator), hybrid nanogenerators, and self-powered nanosystems. He has published over 50 peer reviewed papers, with citation over 1000 and H-index of 19. Details can be found at http://piezotronics.binncas.cn/.

**Dr. Zhong Lin (ZL) Wang** is the Hightower Chair in Materials Science and Engineering, Regents' Professor, at Georgia Tech. He is also the chief scientist and director of Beijing Institute of Nanoenergy and Nanosystems, Chinese Academy of Sciences. Dr. Wang has made original and innovative contributions to the synthesis, discovery, characterization and understanding of fundamental physical properties of oxide nanobelts and nanowires, as well as applications of nanowires in energy sciences, electronics, optoelectronics and biological science. He is the leader figure in ZnO nanostructure research. His discovery and breakthroughs in developing nanogenerators establish the principle and technological road map for harvesting mechanical energy from environment and biological systems for powering a personal electronics. His research on self-powered nanosystems has inspired the worldwide effort in academia and industry for studying energy for micro-nano-systems, which is now a distinct disciplinary in energy research and future sensor networks. He coined and pioneered the field of piezotronics and piezo-phototronics by introducing piezoelectric potential gated charge transport process in fabricating new electronic and optoelectronic devices. This historical breakthrough by redesign CMOS transistor has important applications in smart MEMS/NEMS, nanorobotics, human-electronics interface and sensors. Wang also invented and pioneered the in-situ technique for measuring the mechanical and electrical properties of a single nanotube/nanowire inside a transmission electron microscope (TEM).